# FUNCTIONAL PREDICTIVE CONTROL DESIGN FOR AN ISOLATED WIND GENERATION SYSTEM

Ahmed M. KASSEM[1]

*This paper investigates the application of the model predictive control (MPC) approach to control the voltage and frequency of a stand alone wind generation system. This scheme consists of a wind turbine which drives an induction generator feeding an isolated load. A static reactive power compensator (SVAR) is connected at the induction generator terminals to regulate the load voltage. The rotor speed, and thereby the load frequency are controlled via adjusting the mechanical power input using the blade pitch-angle control. The MPC is used to calculate the optimal control actions including system constraints. To alleviate computational effort and to reduce numerical problems, particularly in large prediction horizon, an exponentially weighted functional model predictive control (FMPC) is employed.*

*Digital simulations have been carried out in order to validate the effectiveness of the proposed scheme. The proposed controller has been tested through step changes in the wind speed and the load impedance. Simulation results show that adequate performance of the proposed wind energy scheme has been achieved. Moreover, this scheme is robust against the parameters variation and eliminates the influence of modeling and measurement errors.*

**Keywords**: wind turbine; induction generator; constrained predictive control; functional model predictive control.

## 1. Introduction

New resources for electricity generation as wind, hydro…etc has been focused in recent years. Induction generator was used as the electromechanical energy converter in such generation schemes. The induction generators have many advantages such as low maintenance cost, robustness, reduced size, good transient performance, absence of moving contacts and no need for DC. excitation. The self excited induction generator (SEIG) is capable of generating electrical energy from constant speed as well as variable speed prime movers. Such an energy system can feed electrical energy to isolated locations, which in turn can enhance agriculture production and improve the standard of living in remote areas. In spite of having several advantages, it has limited applications to power systems due to its poor voltage regulation. The steady state and dynamic performances of an isolated SEIG under various loading conditions have been presented and

[1] Assistant Prof., Dept.of electrical Engineering, Beni-Suef University, Egypt, e-mail: Kassem_ahmed53@hotmail.com

discussed [1-7]. It has been proved that the magnitude of the terminal voltage of a SEIG depends upon the load impedance, excitation capacitance, and speed of the prime mover. On the other hand, the stator frequency of the SEIG depends mainly upon the speed of the prime mover. The suitability of such units for wind generation schemes depends upon the ability of the control system to provide constant voltage at varying loads and different prime mover's speed.

Many investigations have concerned with the voltage and/or frequency control of the wind driven induction generator. Thus, the SVAR was employed to adjust the terminal voltage of the SEIG on the basis of lookup table [8], impedance controller [9-10]. Also, the inverter based reactive power sources [11-12] have been used for regulating the output voltage profile of a SEIG under various loading conditions. In [13-15], the field orientation technique has been employed to keep the dc bus voltage at a constant value by varying the stator flux in the induction generator when the rotor speed is varied. However, PI-controllers; which have poor transient responses; were employed in these control schemes.

Artificial intelligence techniques, such as fuzzy logic, neural network, and genetic algorithms, are recently showing a lot of promise in the application of power electronic systems. Thus, a fuzzy logic controller has been used to enhance the performance of a variable speed wind generation system [16]. Also, a neural network controller has been employed to adapt the value of excitation capacitor [17] based on the steady state analysis of the wind generation system. Nevertheless, these methods couldn't offer good transient performance.

In recent years, many researchers have been used MPC in wind energy conversion [18-22]. The MPC controller generally requires a significant computational effort. As the performance of the available computing hardware has rapidly increased and new faster algorithms have been developed, it is now possible to implement MPC to command fast systems with shorter time steps, as electrical drives. Electric drives are of particular interest for the application of MPC for at least two reasons:

1) They fit in the class of systems for which a quite good linear model can be obtained both by analytical means and by identification techniques;

2) Bounds on drive variables play a key role in the dynamics of the system; indeed, two main approaches are available to deal with system constraints: anti–windup techniques, widely used in the classical PI controllers, and MPC. The presence of the constraint is one of the main reasons why, for example, state space controllers have limited application in electrical drives.

In spite of these advantages, MPC applications to electrical drives are still largely unexplored and only few research laboratories are involved on them. For example Generalized Predictive Control (GPC) – a special case of MPC – has been applied to induction motors for the only current regulation [23] and later for

the speed and current control [24]. In [25], the more general MPC solution has been adopted for the design of the current controller in the same drive.

In this paper a centralized MPC with large prediction horizon for voltage and frequency control of isolated wind-generation system is presented. The proposed centralized scheme improves the control performance in a coordinated manner.

Another challenge of MPC for centralized PMSM is its large computational effort needed. To overcome this drawback, a functional MPC with orthonormal basis Laguerre function [26] is presented. The presented functional MPC reduces computational effort significantly which makes it more appropriate for practical implementation. In addition, an exponential data weighting is used to reduce numerical issue in MPC with large prediction horizon [27]. To verify the effectiveness of the proposed scheme, time-based simulations are carried out. The results obtained proved that the functional MPC is able to control successfully the wind-generation system in the transient and steady state cases.

## 2. System Description And Dynamics

The chapter titles will be numbered, if necessary, and will be written in small characters (12 pts), bold.

The presentation will be clear and concise and the symbols used therein will be specified in a symbol list (if necessary). In the paper it will be used the measurement units International System. In the paper, there will be no apparatus or installation descriptions.

The proposed wind energy conversion system (WECS) is shown in fig. 1, which consists of SEIG driven by wind turbine and feeding isolated load through static VAR compensator. The static VAR compensator used is a fixed-capacitor thyristor-controlled reactor (FCTCR), which is connected at the generator terminals for voltage regulation. In this case, the generator's terminal voltage depends mainly on the static VAR capacitance, rotor speed and the load impedance. The stator frequency depends mainly on the rotor speed. Therefore, if the wind velocity changes, or if the load on the induction generator changes, there is a possibility that the terminal voltage and frequency will change. This is objectionable to sensitive loads. In this paper, the FMPC controller has been suggested to overcome this problem. So, the generator's terminal voltage can be regulated by adjusting the static VAR firing angle $\alpha$ using integral regulating as shown in the following equation:

$$p\alpha = V_{ref} - v_{ds} \tag{1}$$

Where $V_{ref}$, and $v_{ds}$ are the reference and actual voltages at the generator terminals respectively.

To regulate the frequency, the rotor speed must be controlled. The rotor speed can be adjusted by controlling the turbine's output power. The power output of the wind turbine can be adjusted by regulating the blade angle β of the turbine according to the following differential equation:

$$P\beta = P_{ref} - P_t \tag{2}$$

Where $P_t$ is the turbine output power, which is a function in the blade angle, rotor speed, and wind speed as shown below.

$$P_t = \frac{1}{2}\rho A C_p V_w^3$$

Where $\rho$ is the air density, and $A$ is the swept area by the blades [28], and

$$C_p = (0.44 - 0.0167\beta)\sin\frac{\pi(\lambda - 3)}{15 - 0.3\beta} - 0.00184(\lambda - 3)\beta$$

The value of the reference power is chosen at rated wind speed, optimal tip-speed ratio and zero blade angle.

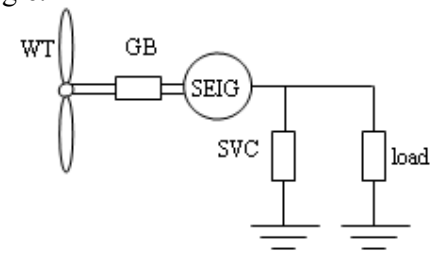


Fig.1. Schematic representation of the wind energy system

### *2.1. Complete System Dynamic and Linearized Model*

Then, the complete dynamic model of the proposed isolated wind-generation system can be described as follows [9] and [29]:

$$pi_{qs} = -R_s A_1 i_{qs} - (\frac{i_{qs} - i_{qLo} - i_{qL}}{C_o V_{ds}} + A_2 \omega_m L_m) i_{ds} + R_r A_2 i_{qr} - A_1 \omega_m L_r i_{dr} \tag{3}$$

$$pi_{ds} = (\frac{i_{qs} - i_{qLo} - i_{qL}}{C_o V_{ds}} + A_2 \omega_m L_m) i_{qs} - R_s A_1 i_{ds} + R_r A_2 i_{dr} + A_1 \omega_m L_m i_{qr} - A_1 v_{ds} \tag{4}$$

$$pi_{qr} = R_s A_2 i_{qs} + A_2 \omega_m L_s i_{ds} - A_3 i_{qr} + (-\frac{i_{qs} - i_{qLo} - i_{qL}}{C_o V_{ds}} + A_1 \omega_m L_s) i_{dr} \tag{5}$$

$$pi_{dr} = -A_2 \omega_m L_s i_{qs} + R_s A_2 i_{ds} + (\frac{i_{qs} - i_{qLo} - i_{qL}}{C_o V_{ds}} - A_1 \omega_m L_s) i_{qr} - A_3 i_{dr} + A_2 v_{ds} \tag{6}$$

$$p\omega_m = (-f\omega_m + PT_m + 1.5P^2 L_m (i_{qs} i_{dr} - i_{ds} i_{qr}))/J \tag{7}$$

$$pv_{ds} = \frac{\dot{\boldsymbol{i}}_{ds} - i_{dLo} - i_{dL}}{C_o} \tag{8}$$

$$Pi_{qL} = \frac{1}{L}\left[ - R\, i_{qL} - \left( \frac{i_{qs} - i_{qLo} - i_{qL}}{C_o\ v_{ds}} \right)\ L\, i_{dL} \right] \tag{9}$$

$$Pi_{dL} = \frac{1}{L}\left[ v_{ds} - R\, i_{dL} + \left( \frac{i_{qs} - i_{qLo} - i_{qL}}{C_o\ v_{ds}} \right) L\ \ i_{qL} \right] \tag{10}$$

$$pi_{qLo} = -\left( \frac{i_{qs} - i_{qLo} - i_{qL}}{C_o\ V_{ds}} \right) i_{dLo} \tag{11}$$

$$pi_{dLo} = \frac{v_{ds}}{L_{eq}} + \left( \frac{i_{qs} - i_{qLo} - i_{qL}}{C_o\ V_{ds}} \right) i_{qLo} \tag{12}$$

$$p\alpha = V_{ref} - v_{ds} \tag{13}$$

$$P\beta = P_{ref} - P_t \tag{14}$$

In this paper, the linear model predictive controlled is used, so it is assumed that the plant dynamics are linear. Therefore, small signal linear model of the proposed WECS is linearized around an operating point to study the system dynamics when subjected to small perturbations. The linearized model can be described by the following equation:

$$px = Ax + B\mu + \eta\nu \tag{15}$$

Where

$x = [\Delta i_{qs}\ \Delta i_{ds}\ \Delta i_{qr}\ \Delta i_{dr}\ \Delta\omega_m\ \Delta v_{ds}\ \Delta i_{ql}\ \ \Delta i_{dl}\ \Delta i_{qlo}\ \Delta i_{dlo}\ \Delta\alpha\ \Delta\beta]^t$ , $\mu = \begin{bmatrix} V_{ref} & P_{ref} \end{bmatrix}^t$ ,

$\nu = \begin{bmatrix} \Delta V_w & \Delta Z_L \end{bmatrix}^t$

Where $x$ represents system states variables, $\mu$ represents control inputs, $\nu$ represents the disturbance.

Also, $A = [\,a_{ij}\,]$ is a 12 x 12 matrix containing the system parameters.

## 3. Functional Model Predictive Control

### *3.1. Model predictive Control*

Model predictive control uses an explicit model of system to predict future trajectory of system states and outputs. This prediction capability allows solving optimal control problem online, where prediction error (i.e. containing difference between the predicted output and reference output) and control input action are minimized over a future horizon, possibly subject to constraints on the manipulated inputs, states and outputs. The optimization yields an optimal control sequence as input and only the first input from the sequence is used as the input to

the system. At the next sampling interval, the horizon is shifted and the whole optimization procedure is repeated. The main reason for using this procedure, which is called receding horizon control (RHC), is that it allows compensating for future disturbance and modeling error.

The basic structure of model predictive control is depicted in Fig. 2. An explicit model of the system is used to predict future output response chain $\hat{y}$. Based on the predicted system output and current system output, the error is calculated. The errors, then, are fed to the optimizer. In the optimizer, the future optimal control sequence, $\Delta u$, is calculated based on the objective function and system constraints.

In this paper, the state space model of the system is used in the model predictive control. The general discrete form of the state space model used in model predictive control is of the form:

$$\begin{aligned} x(k+1) &= A_z x(k) + B_z u(k) + E_z d(k) + F_z w(k) \\ y(k) &= C_z x(k) \end{aligned} \tag{16}$$

where $k$ is the sampling instant, $x$ is state vector, $u$ is input vector, d represents system disturbance and $w$ represents system noise model. $A_z$, $B_z$, $C_z$, $E_z$ and $F_z$ are coefficients of system state space model and reflect the isolated wind generation system model in (15).

The final aim of model predictive control is to provide zero output error with minimal control effort.

Therefore, the cost function $J$ that reflects the control objectives, is defined as:

$$J(n) = \sum_{k=1}^{N_p} \mu_k \left( y'(n+k) - y_{ref}(n+k) \right)^2 + \sum_{k=1}^{N_c} v_k \Delta u(n+k)^2 \tag{17}$$

Where

$\mu_k$ *and* $v_k$ respectively, the weighting factors for the prediction error and control energy;

$y'(n+k)$ $k^{th}$ step output prediction;

$y_{ref}(n+k)$ $k^{th}$ step reference trajectory;

$\Delta u(n+k)$ $k^{th}$ step control action.

where the first term reflects the future output error and second term reflects the consideration given to the control effort. The predicted output vector has dimension of $1 \times N_p$ where $N_p$ is the prediction horizon. $\Delta u$ is control action vector with dimension of $1 \times Nc$ that $N_c$ is control horizon. In the model predictive control, the control horizon, $N_c$ , is always smaller than or equal to prediction horizon ($N_p$ ). $\mu_k$ *and* $v_k$ reflecting the weights on the predicted error of predicted outputs and change in the control action.

The constraints of model predictive control include constraints of magnitude and change of input, state and output variables that can be defined in the following form.

$$\begin{aligned} &u_{\min} \le u(n+k) \le u_{\max}, \quad && \Delta u_{\min} \le \Delta u(n+k) \le \Delta u_{\max} \\ &x_{\min} \le x(n+k) \le x_{\max}, \quad && \Delta x_{\min} \le \Delta x(n+k) \le \Delta x_{\max} \\ &y_{\min} \le y(n+k) \le y_{\max}, \quad && \Delta y_{\min} \le \Delta y(n+k) \le \Delta y_{\max} \end{aligned} \tag{18}$$

Solving the objective function (17) with system constraint (18) gives the optimal input control sequence.

### *3.2. Laguerre Based MPC*

In the classical model predictive control, the future control signal is modeled as a vector of forward shift operator with length of *Nc* .

$$\Delta U = \left[\Delta u(n),...,\Delta u(n+k),...,\Delta u(n+N_c-1)\right] \tag{19}$$

where $N_c$ unknown control variables are achieved in the optimization procedure. When large prediction horizon is needed to achieve high closed loop performance that needs large computational burden. Therefore, MPC may not be fast enough to be used as a real time optimal control for such case.

A solution to this drawback is using functional MPC. In the functional MPC, future input is assumed to be a linear combination of a few simple base functions. In principle, these could be any appropriate functions. However in practice, a polynomial basis is usually used [30]. This approximation of input trajectory can be more accurate by proper selection of base function. Using functional MPC, the term used in the optimization procedure can be reduced to a fraction of that required by classical MPC. Therefore, the computational load will be reduced largely.

In this paper, orthonormal basis Laguerre function is used for modeling input trajectory. Laguerre polynomial is one of the most popular orthonormal base functions which has extensive applications in system identification [26]. The z-transform of *m'th* Laguerre function is given by:

$$\Gamma_m = \frac{\sqrt{1-a^2}}{z-a}\left[\frac{1-az}{z-a}\right]^{m-1} \tag{20}$$

where *0≤a≤1* is the pole of Laguerre polynomial and is called scaling factor in the literature. The control input sequence can be described by the following Laguerre functions:

$$\Delta u(n+k) \approx \sum_{m=1}^{N} c_m\, l_m(k) \tag{21}$$

where $l_m$ is the inverse z-transform of $\Gamma_m$ in the discrete domain. The coefficients $c_m$ are unknowns and should be obtained in the optimization procedure. The parameters *a* and *N* are tuning parameters and should be adjusted by user. Usually the value of *N* is selected smaller than 10 that is enough for most practical

applications. Generally, choosing larger value for $N$ increases the accuracy of input sequence estimation.

### *3.3. Exponentially Weighted MPC*

Closed loop performance of MPC depends on the magnitude of prediction horizon $N_p$. Generally, by increasing the magnitude of prediction horizon, the closed loop performance will be improved. However, practically, selection of large prediction horizon is limited by numerical issue, particularly in the process with high sampling rate. One approach to overcome this drawback is to use exponential data weighting in model predictive control [27].

### *3.4. Design of the proposed Functional Model Predictive Control*

In this section, the Laguerre based model predictive control and exponentially weighted model predictive control are combined in order to alleviate computational effort and reduce numerical problems. At first, a discrete model predictive control with exponential data weighting is designed. The input, state and output vectors are changed in the following way:

$$\begin{aligned}
\Delta\hat{U}^T &= \left[\sigma^{-0}\Delta u(n),...,\sigma^{-(N_c-1)}\Delta u(n+N_c-1)\right] \\
\hat{X}^T &= \left[\sigma^{-1}x(n+1),...,\sigma^{-N_p}x(n+N_p)\right] \\
\hat{Y}^T &= \left[\sigma^{-1}y(n+1),...,\sigma^{-N_p}x(n+N_p)\right]
\end{aligned} \tag{22}$$

where $\sigma$ is tuning parameter in exponential data weighting and is larger than 1. The state space representation of system with transformed variable is:

$$\begin{aligned}
\hat{x}(n+1) &= \hat{A}\,\hat{x}(n) + \hat{B}\,\Delta\hat{u}(n) \\
\hat{y}(n) &= \hat{C}\,\hat{x}(n)
\end{aligned} \tag{23}$$

Where $\hat{A} = A/\sigma$ , $\hat{B} = B/\sigma$ , $\hat{C} = C/\sigma$

The optimal control trajectory with transformed variables can be achieved by solving the new objective function and constraints.

$$\hat{J}(n) = \sum_{k=1}^{N_p} \mu_k \left(\hat{y}(n+k) - y_{ref}(n+k)\right)^2 + \sum_{k=1}^{N_c} \nu_k \Delta\hat{u}(n+k)^2 \tag{24}$$

$$\begin{aligned}
&\sigma^{-k}u_{\min} \le \hat{u}(n+k) \le \sigma^{-k}u_{\max} \;,\; \sigma^{-k}\Delta u_{\min} \le \Delta\hat{u}(n+k) \le \sigma^{-k}\Delta u_{\max} \\
&\sigma^{-k}x_{\min} \le \hat{x}(n+k) \le \sigma^{-k}x_{\max} \quad , \quad \sigma^{-k}\Delta x_{\min} \le \Delta\hat{x}(n+k) \le \sigma^{-k}\Delta x_{\max} \\
&\sigma^{-k}y_{\min} \le \hat{y}(n+k) \le \sigma^{-k}y_{\max} \quad , \quad \sigma^{-k}\Delta y_{\min} \le \Delta\hat{y}(n+k) \le \sigma^{-k}\Delta y_{\max}
\end{aligned} \tag{25}$$

By choosing $a>1$, the condition number of hessian matrix will be reduced significantly, especially for large values of prediction horizon ($N_p$).This leads to a more reliable numerical approach.

After solving new objective function with new variables, the calculated input trajectory should be transformed into standard variable with the following equation.

$$\Delta U^T = \left[a^o \Delta\hat{u}(k), \ldots, a^{(N_c-1)} \Delta\hat{u}(k+N_c-1)\right] \tag{26}$$

The Laguerre based model predictive control and exponentially weighted model predictive control can be combined using the following systematic procedure:

- Choosing of the proper tuning parameter σ .
- Transforming the system parameters (A, B, C) and the system variables (U, X, Y) are transformed using equations (23) and (24).
- The objective function with its constraints is created based on equations (25) and (26).
- Optimizing objective function based on Laguerre polynomial and then calculating unknown Laguerre coefficients.
- Calculating input chain from equation (21).

The calculated weighted input chain is transformed into unweighted input chain using equation (26) and applied on the plant.

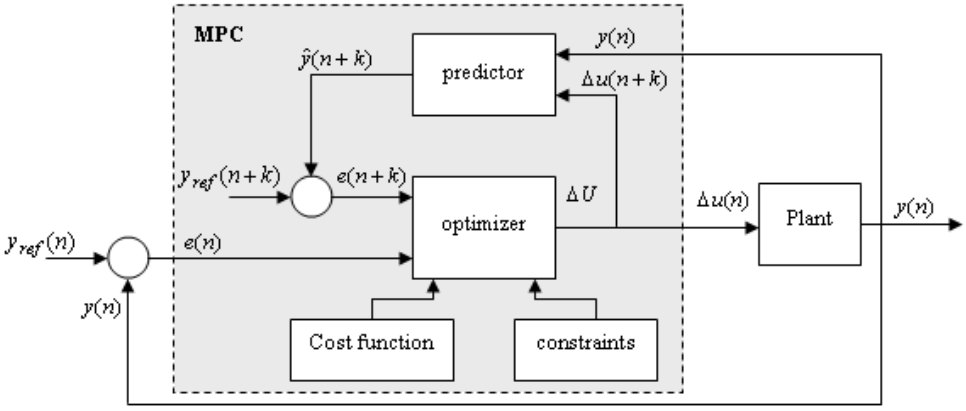


Fig. 2. Basic structure of model predictive control

## 4. System Configuration

Fig. 3 shows the block diagram of the WECS with the proposed FMPC controller. There are two paths of control are used here based on FMPC to regulate load voltage and frequency. The first path is dedicated for regulating the terminal voltage of the induction generator to a reference value via adjusting the firing angle of the thyristor of the SVAR. The second path is used to control the

mechanical input power to the generator by adjusting the blade pitch angle of the wind turbine. A blade pitch actuator is used to control the mechanical power and hence the system rotational speed and consequently the terminal voltage frequency.

Digital simulations are obtained to validate the performance of the proposed FMPC with the isolated WECS. The input to the FMPC is the terminal voltage error and the generator's input power error. And the output of the FMPC is considered as TCR firing angle and the blade angle. The control parameters are assumed as following

input weight matrix: $\mu=0.18\times I_{Nc\times Nc}$

output weight matrix: $v=1\times I_{Np\times Np}$

The constraints are chosen such that, the TCR firing angle is normalized to be between 0 and 1, where 0 corresponds to $(\alpha_{\min})$ and 1 corresponds to maximum firing angle $(\alpha_{\max})$. Also, the blade angle is normalized to be between 0 and 1, where 0 corresponds to $\beta_{\min}=0$ and 1 corresponds to maximum blade angle ( $\beta_{\max}$), thus:

$$\begin{bmatrix}\alpha_{\min}\\ \beta_{\min}\end{bmatrix}=0\le u\le 1=\begin{bmatrix}\alpha_{\max}\\ \beta_{\max}\end{bmatrix}.$$

The constraints imposed on the control signal are hard, whereas the constraints on the states are soft, i.e., small violations can be accepted. The constraints on the states are chosen such that to guarantee signals stay at physically reasonable values as follows:

$$x_{\min}=\begin{pmatrix}0\\0\\0\\0\\0\\0\end{pmatrix}\le\begin{pmatrix}|i_{qs}|\\|i_{ds}|\\|\omega_r|\\|v_{ds}|\\|i_{ql}|\\|i_{dl}|\end{pmatrix}\le\begin{pmatrix}8\\3\\400\\140\\2\\1.2\end{pmatrix}=x_{\max}$$

The entire system has been simulated on the digital computer using the Matlab / Simulink /software package. The specifications of the system used in the simulation procedure are listed in appendix [29]:

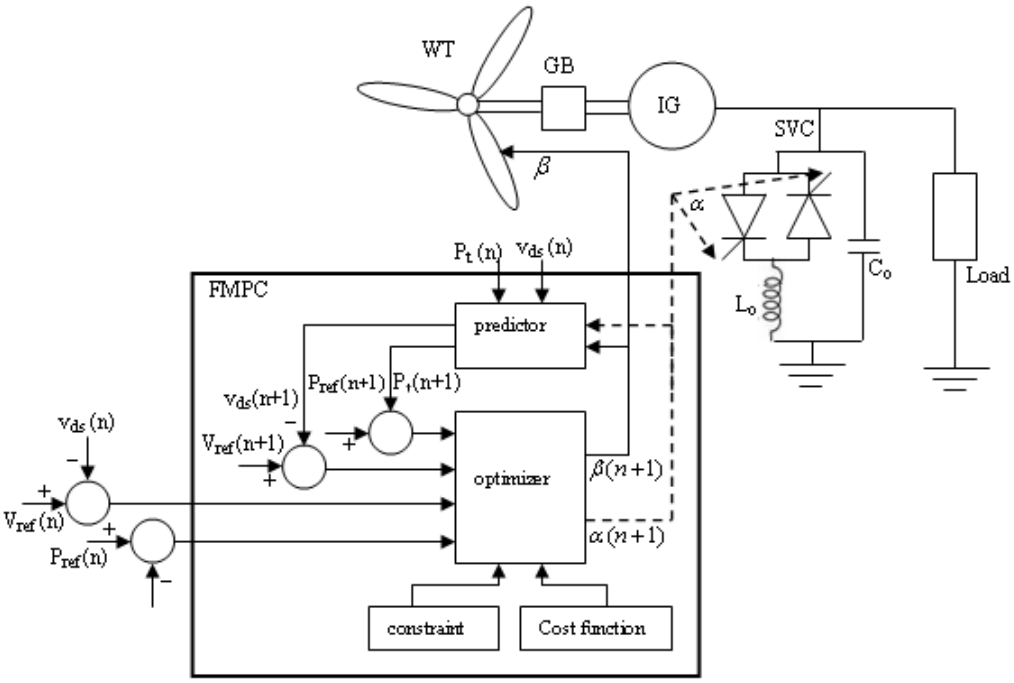


Fig. 3. Block diagram of the wind energy conversion system with the proposed FMPC controller

## 5. Simulation Results

Digital simulations have been carried out to validate the effectiveness of the proposed system under load and wind velocity excursions. The parameters of the FMPC based on Laguerre function are adjusted to be $a=0.27$, $N=6$, $\sigma=1.08$, $N_p=300$ and $N_c=5$.

The performance of the proposed scheme has been tested with a turbulence change in wind speed. In addition, the system response is investigated during a step change of load impedance.

Simulation results depicting the variation of different variables with step turbulence in wind speed are shown in Fig. (4). The wind speed is assumed to vary between 6 m/s and 8 m/s. It has been noticed that as the wind velocity increases, the firing angle of the thyristor will decrease. This is because, at higher wind speed, the shaft torque output of the wind turbine increases and tends to increase the rotor speed of the induction generator. The control action can be summarized as follows:

a) If the terminal voltage tends to increase due to the increase in wind speed, the FMPC controller comes into operation and decreases the firing angle of the thyristor. This would result in reducing the equivalent inductance of the reactor in

the SVAR and, in turn, increasing the reactor current. Consequently, the total effective load on the induction generator will increase. The terminal voltage tends to reduce and settles down to the reference value.

b) If the electrical frequency of the generator tends to increase due to the increase in wind speed, the controller will increase the blade angle causing the mechanical input power to decrease. This will reduce the rotor speed and so the terminal frequency.

c) If the terminal voltage and /or frequency tries to decrease due to reduced wind velocity, the controller will take an action which is opposite to that outlined above.

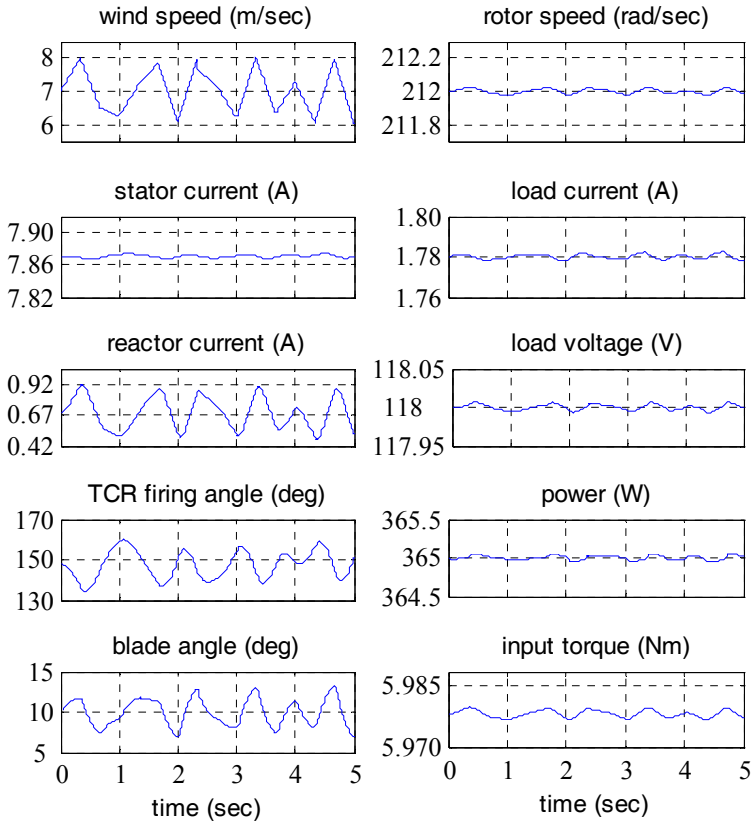


Fig. 4. Simulation results of the proposed scheme with step change in wind speed

Fig. 5 shows simulation results of the proposed system with step change in load impedance. It is seen that the action of the FMPC controller, with a step

increase in load impedance (or a decrease in load current ) is similar to that with an increase in wind velocity and vice versa. Thus, if the load impedance is assumed to be abruptly increased, the load current will decrease. In response to the load reduction, the terminal voltage tend to rise. Therefore, the proposed controller comes into action and decreases the firing angle of the thyristor. This is, in turn, will increase the reactor current causing the effective load on the induction generator to increase, and in turn, the terminal voltage to restore its reference. Also, reduction in load current leads to increase in rotor speed and hence in the electrical frequency of the generator, so the controller will increase the blade angle causing the mechanical input power to decrease. This will reduce the rotor speed and so the terminal frequency.

On the other hand, if the load impedance decreases, the controller increases the thyristor firing angle which decreases the reactor current and decreases the blade angle to compensate for the load increase.

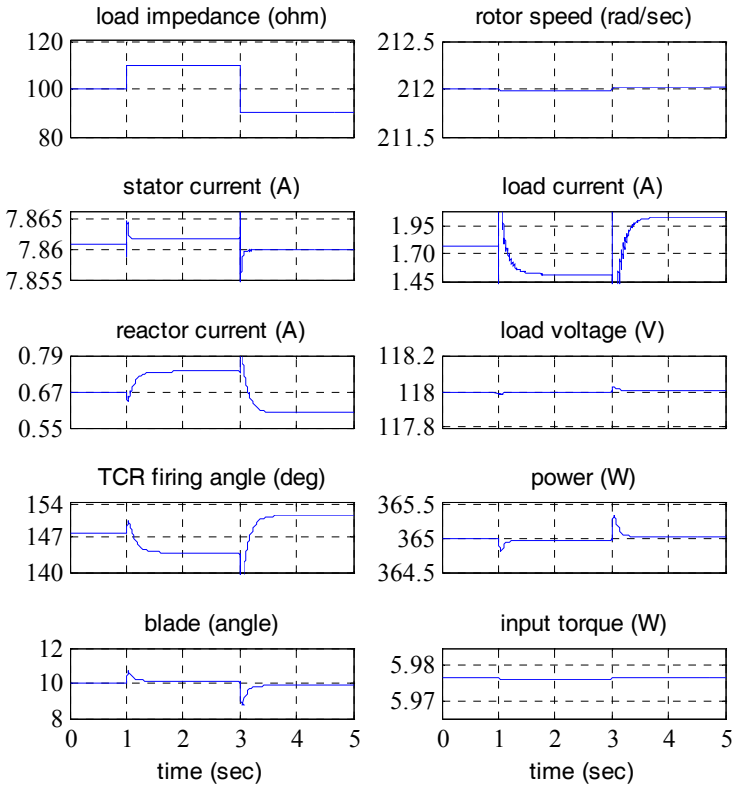


Fig. 5. Simulation results of the proposed scheme with step change in load impedance.

### *5.1. Robustness*

Since our concerns are also in robust stability against various model uncertainties, some system parameters have been changed as follows:

i) The stator and rotor resistances are assumed to increase by 20% above nominal values.
ii) The moment of inertia is assumed to rise 20% above nominal.
iii) The magnetizing inductance is assumed to be 10% less than nominal.

For perturbed system the responses are shown in fig. 6 and fig. 7. It should be seen that the system is robustly stable in spite of parameters variations.
It has been indicated in the figures that the FMPC controller is able to stabilize the terminal voltage and frequency with high accuracy in spite of modeling errors.

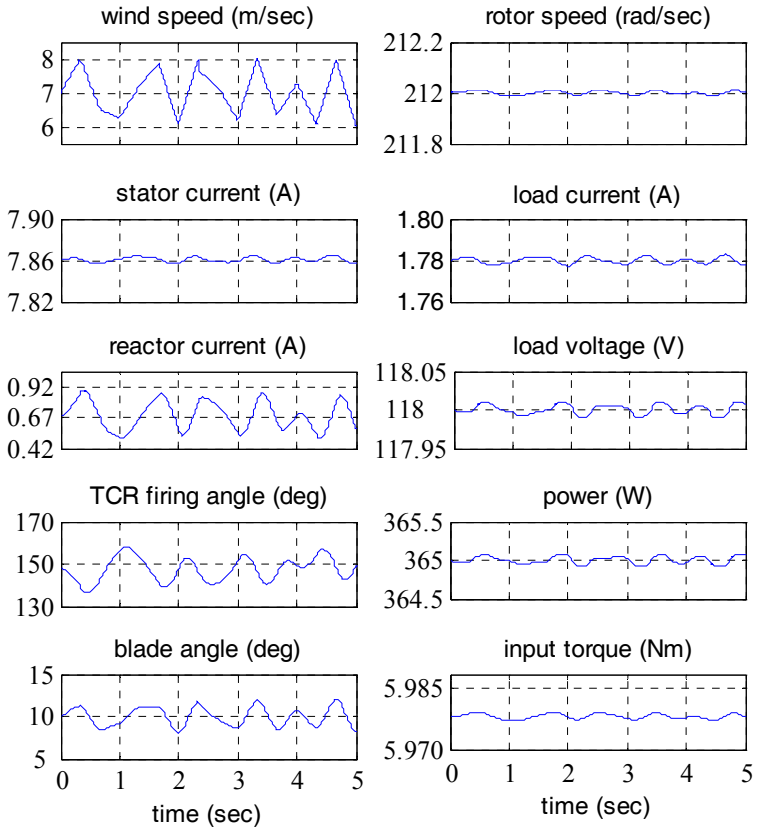


Fig. 6. Simulation results of the proposed scheme with step change in wind speed with parameters change.

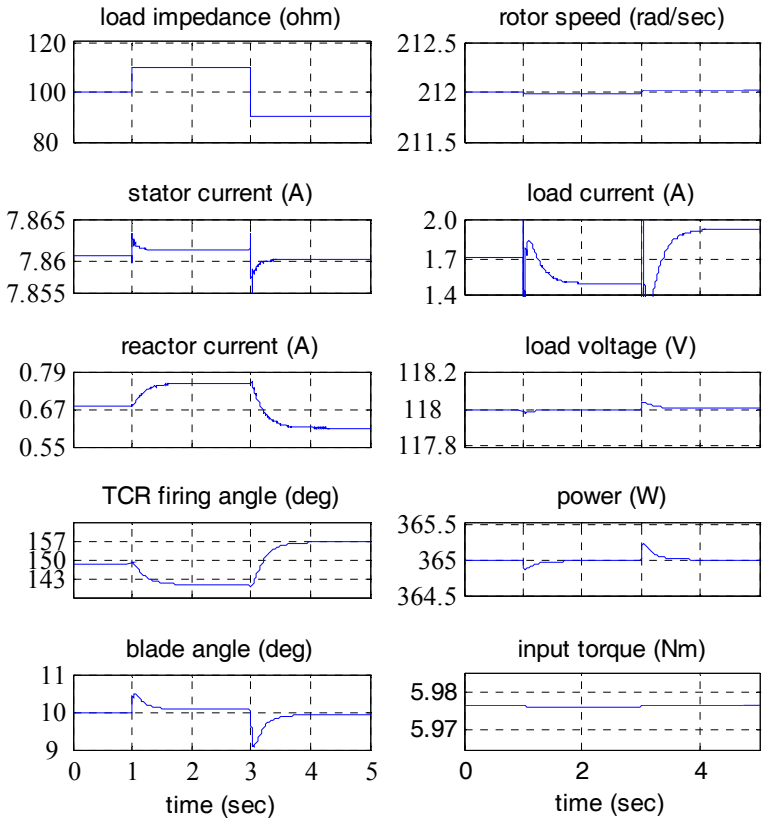


Fig. 7. Simulation results of the proposed scheme with step change in load impedance with parameters change.

## 6. Conclusions

This paper investigates the robust centralized functional model predictive controller to control the terminal voltage and frequency of a SEIG. The SEIG driven by wind turbine and feeding static load. This scheme consists of a wind turbine, induction generator, SVAR compensator (fixed capacitor in parallel with thyristor controlled reactor), and static load. The firing angle of the thyristor is controlled according to the error between the reference and actual load voltages. Also, the rotor speed is adjusted by controlling the blade pitch-angle according to the error between the reference and actual mechanical power input to the generator. The complete nonlinear dynamic model of the system has been described and linearized around an operating point.

The proposed predictive controller uses orthonormal Laguerre functions to describe control input trajectory which reduces real time computation largely. Also, exponential data weighing is used to decrease numerical issue, particularly in large prediction horizon. Constraints are imposed on both the TCR firing angle and the blade angle.

Digital simulations have been carried out in order to evaluate the effectiveness of the proposed scheme. The wind energy system with the proposed controller has been tested through turbulence changes in wind speed and step changes in load impedance. The results prove that the proposed controller is successful in regulating the terminal voltage and frequency of a stand alone wind energy conversion system under wind and /or load excursion and it is robust against system parameters change.

NOMENCLATURE

| | |
|---|---|
| $v_{ds}$ , $v_{qs}$ | d-q stator voltages, |
| $i_{ds}$, $i_{qs}$ | d-q stator currents, |
| $i_{dr}$, $i_{qr}$ | d-q rotor currents, |
| $R_s$, $R_r$ | stator and rotor resistances per phase, |
| $L_s$, $L_r$, $L_m$ | stator, rotor and magnetizing inductances |
| $C_0$ | self excitation capacitance per phase, |
| $\omega_s$ | angular stator frequency of the induction generator, |
| $\omega_m$ | angular rotor speed (electrical rads/sec) of the induction generator, |
| $\omega_t$ | angular rotor speed of the turbine, |
| $J$ | moment of inertia, |
| $f$ | friction coefficient, |
| $p$ | differential operator *d/dt* , |
| $L_o$ | physical inductance of the reactor in the SVAR, |
| $\alpha$ | firing angle of the SVAR, |
| β | Turbine blade pitch angle, |
| $i_{dL}$, $i_{qL}$ | d-q load current, |
| $i_{dLo}$, $i_{qLo}$ | d-q reactor current in the SVAR, |
| λ | turbine tip speed ratio, |
| $P$ | number of pole pairs. |

## R E F E R E N C E S

[1] *J. Sallan, E. Muljadi, M. Sanz and C. P. Butterfield*, "Control of self-excited induction generators driven by wind turbines" IEEE Trans. on Energy Conversion, Vol. 12, 2000.

[2] *T.F. Chan and Loi Lei Lai,* " steady-state analysis and performance of a stand-alone three-phase induction generator with asymmetrically connected load impedances and excitation capacitances". IEEE Trans. On Energy Conversion, Vol. 16, No. 4, Dec., 2001, pp 91-96.

[3] *T.F. Chan*, "Steady-state analysis of self-excited induction generators" IEEE Trans. on Energy Conversion, Vol. 9, No. 2, p 288-296, June1994.

[4] *E. Muljadi, J. Sallan, M. Sanz and C. P. Butterfield*, "Investigation of self-excited induction generators for wind turbine applications" IEEE Trans. on Energy Conversion, Vol. 12, 2000

[5] *C. Chakraborty, S. N. Bhadra and A. K. Chattopadhyay*, "Excitation requirements for stand alone three-phase induction generator" IEEE Trans. on Energy Conversion, Vol. 13, No. 4, p 358-365, December 1998.

[6] *Li Wang, and J. Su*, " Dynamic performances of an isolated self excited induction generator under various loading conditions", IEEE Trans. on Energy Conversion, Vol. 14, No.1, p. 93-102, March 1999.

[7] *Kassa Idjdarene, Djamila Rekioua, Toufik Rekioua, and Abdelmouna¨ım Tounzi*, "Performance of an isolated induction generator under unbalanced loads". IEEE TRANSACTIONS ON ENERGY CONVERSION, VOL. 25, NO. 2, JUNE 2010, pp 303-311.

[8] *A.A. Shaltout and M.A. Abd el-Halim*, "Solid-state control of a wind-driven self-excited induction generator". IEEE Electric Machines and Power System, Vol. 23, p 571-582, 1995.

[9] *R.M. Hilloowala*, " Control and interface of renewable energy systems", Ph.D. Thesis, The University of New Brunswick, Canada, 1992.

[10] *R. Bonert and S. Rajakaruna*, "Self-excited induction generator with excellent voltage and frequency control", IEE Proc.- Gener. Transm. Distrib., Vol. 145, No 1, p 33-39, January 1998.

[11] *E.G. Marra, and J.A. Pomilio*, " Self-excited induction generator controlled by a VS-PWM bidirectional converter for rural applications", IEEE Trans. on Industrial Applications, Vol. 35, No. 4, July/August 1999.

[12] *S.C. Kuo and L. Wang*, "Analysis of voltage control for a self-excited induction generator using a current-controlled voltage source inverter (CC-VSI)" IEE Proc. Gener. Transm. Distrib., Vol. 148, No. 5, p 431-437, September 2001.

[13] *D. Seyoum, M. Rahman, and C. Grantham*," Terminal voltage control of a wind turbine driven isolated induction generator using stator oriented field control", Proc. Of the IEEE Eighteenth Annual Applied Power Electronics Conference and Exposition, Vol. 2, Feb. 2003, pp 846-852.

[14] *B.A. Zahir, J. G. Kettleborough and I. R. Smith*, "a stand alone induction generator model producing a constant voltage constant frequency output". IEEE 4th International Conference on Emerging Technologies, Vol. 1, 2008, pp 83-86.

[15] *D.G. Forchetti, J.A. Solsona, G.O. Garc and M.I. Valla*, " A control strategy for stand-alone wound rotor induction machine". Electric Power Systems Research , Vol. 77, pp 163–169, 2007.

[16] *Lotfi Krichen, Bruno Francois and Abderrazak Ouali*, "A fuzzy logic supervisor for active and reactive power control of a fixed speed wind energy conversion system". Electric Power Systems Research, Vol. 78, pp 418–424, 2008.

[17] *A.A. Hassan, Y.S. Mohamed and A. M. Kassem*," A neural voltage regulator for a wind driven self excited induction generator", MEPCON'2003, IEEE, Shebin EL-Kom, , 9th international Middel-East Power Systems Conference, Dec. 16-18, 2003, p. 691 .

[18] *M. Rivera, J L. Elizondo, M.E. Macías, O.M. Probst, O.M. Micheloud, J. Rodriguez, C. Rojas and A. Wilson*, "Model Predictive Control of a Doubly Fed Induction Generator with an

Indirect Matrix Converter". IEEE 36th Annual Conference on Industrial Electronics Society, Nov. 2010, pp 2959-2965.
[19] *Mostafa Soliman, O.P. Malik, and David T. Westwick*, "multiple model predictive control for wind turbines with doubly fed induction generators". IEEE TRANSACTIONS ON SUSTAINABLE ENERGY, VOL. 2, NO. 3, JULY 2011, pp 215-225.
[20] *E.B. Muhando, T. Senjyu, K. Uchida, H. Kinjo and T. Funabashi*, "Stochastic inequality constrained closed-loop model-based predictive control of MW-class wind generating system in the electric power supply". IET Renewable Power Generation, Vol. 4, No 1, 2010, pp 23-35.
[21] *Dawei Zhi, Lie Xu and Barry W. Williams*, " model-based predictive direct power control of doubly fed induction generators". IEEE Transactions On Power Electronics, Vol. 25, No. 2, FEBRUARY 2010.
[22] *Yongchang Zhang, Jianguo Zhu and Jiefeng Hu*, " model predictive direct torque control for grid synchronization of doubly fed induction generator". 2011 IEEE International Electric Machines & Drives Conference, 2011, pp 765-770.
[23] *L. Zhang, R. Norman, and W. Shepherd*, "Long–Range Predictive Control of current regulated PWM for induction motor drives using the synchronous reference frame," IEEE Transactions on Control System. Technology., vol. 5, no. 1, pp. 119–126, 1997.
[24] *R. Kennel, A. Linder, and M. Linke*, "Generalized predictive control (GPC) – ready for use in drive applications?" in Proc. of the IEEE Power Electronics Specialists Conference PESC '01, pp. 1839–1844, 2001.
[25] *A. Linder and R. Kennel*, "Model predictive control for electrical drives," in Proc. of the IEEE Power Electronics Specialists Conference PESC '05, pp. 1793–1799, 2005.
[26] *L. Wang*, Discrete model predictive control design using Laguerre functions. Journal of Process Control, pp. 131-142, 2004.
[27] *L. Wang*, Use of exponential data weighting in model predictive control design. Proc 40th IEEE Conf. on Decision and Control, 2001.
[28] *A. Abdin and X. Wilson*, " Control design and dynamic performance analysis of a wind turbine-induction generator unit", IEEE Trans. On Energy Conversion, Vol. 15, No. 1, March, 2000, pp 91-96.
[29] *Ahmed M. Kassem*, " Advanced control techniques for regulating the voltage and frequency of a wind driven induction generator". PhD thesis, Assuit University, 2006.
[30] *J.M. Maciejowski*, Predictive Control with Constraints, Pearson Education, POD, 2002.

## APPENDIX

SYSTEM PARAMETERS

Wind turbine :

Rating : 1 kw , 450 rpm ( low speed side ) at $V_w$ = 12 m/s .

Size : Height = 4 m , Equator radius = 1 m , Swept area = 4 m2 , $\rho$ = 1.25 kg/ m2.

Induction machine :

Rating : 3-phase , 2 kw , 120 V , 10 A , 4-pole , 1740 rpm .

Parameters : $R_s$ = 0.62 $\Omega$ , $R_r$ = 0.566 $\Omega$ , $L_s$ = $L_r$ = 0.058174 H., $L_m$ = 0.054 H, $J$ = 0.0622 kg.m2 , $f$ = 0.00366 N.m./rad/s.

FC-TCR : $C_o$ = 176 μF , $L_o$ = 0.127 H.